ISSN: 0974-5823 Vol. 7 No. 4 April, 2022

International Journal of Mechanical Engineering

SURFACE MICRO-MACHINED ACCELEROMETER

Dr. D V Manjunatha[1]

Mayya Sharath kumar[2], Akshatha Y E[3], Akshaya Kumar[4], Gulbi Gouri Shanker[5],

[1]Senior Professor and Head of Dept. Of ECE

[2345]Students, Department of Electronics and communication Engineering

Alva's Institute of Engineering and Technology

Affiliated to VTU, Belgaum, Approved By AICTE, New Delhi, Recognized by Govt of Karnataka

Moodbidri 574225, D.K

Abstract - This paper tells the best way to demonstrate a COMSOL microfabricated surface accelerometer (SAM), utilizing electromechanical interface. The model depends working for this issue study an assortment of mathematical building squares can be put away in a source model document as after effects. From there on, other model documents can reuse similar structure blocks by connecting to the aftereffects on the record of source model. Every aftereffect may get contentions to be produce a structure block with explicit aspects or number of highlights. A SAM is made up of three blocked structures in which, two of them are utilized on various occasions by calling the comparing results with various contentions. Vaganova invented the first accelerometer using Micro-Electro–Mechanical System (MEMS) in 1975, according to Middelhoek. MEMS accelerometers advanced significantly in their development because they satisfied the requirements for low-cost, small-size airbag systems with high constancy and capacity to detect the precise acceleration shock produced by a car accident). A MEMS accelerometer was first installed in an automobiles in 1990, and over 100 million accelerometers were sold in 2007. MEMS accelerometers are becoming more common in portable gadgets and play stations to detect changes in their positions. Less area, weight, cheap cost, low power, and easy integration with semiconductors are only a few of the advantages of MEMS accelerometers. [1].

Keywords- surface micro-machined accelerometer, gyroscope, and inertial measurement unit.

I. INTRODUCTION

The Normal pendulum moves to and froth when a nudge is given, it acquires stability after certain time period. Whereas self-balancing bot uses inverted pendulum which cannot attain stable on its own. It simply falls. To prevent the robot from falling, we will be using inverted pendulum algorithm. The idea is to keep the position of the robot upright by countering the forward and backward fall [2]. If the robot starts to fall towards the front, we need to get the motors running forward, if it falls backwards, we need to get the motor running backwards. For that purpose, we will be using the IMU which consists of accelerometer and gyroscope.

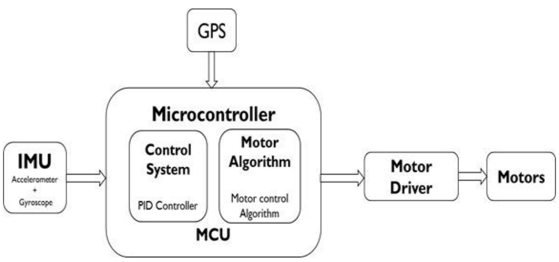

Fig 1.1 Block diagram of self-balancing dairy bot

Inertial measurement unit (IMU) is an electrical device that measures and analyses a body's specific power using a composite of accelerometers, gyrators, and occasionally magnetometers, rakish rate, and occasionally the direction of the body. IMUs are most commonly used to move aeroplanes (a mindset and heading reference framework), such as automated flying vehicles (UAVs), and rockets, such as satellites and landers. The development of IMU-powered GPS devices is being taken into account in current advancements [3]. When GPS signals are unavailable, such as in burrows, inside structures, or when electrical blockage is present, an IMU allows a GPS collector to work.

In inertial navigation systems, accelerometers and gyroscopes work together. Modern automotive airbag deployment systems are one of the most prevalent applications for MEMS accelerometers. Accelerometers are widely utilised in a wide range of applications, including everything from vehicle airbag systems to toys and household goods. The emergence of the supporting technology known as "Micro-electromechanical systems," or MEW, which dropped the cost of producing accelerometers from $250 to under $2 in less than a decade, paved the way for wider deployment. The spring–mass–damp system can be used to describe a micromachined accelerometer to first-order approximation. In this study, accelerometers are used as a vehicle to investigate the various components of surface micromachined sensors. We begin with a brief examination of detecting variables for straight speed improvement and their recommendations for estimation framework execution. The setting for a description of a particular methodology developed at Berkeley is an outline of the few methodologies for co-manufacture of polysilicon microstructures and CMOS. Then there's a discussion of capacitive position detecting circuits and their drawbacks. The use of closed circle sensor structures is then investigated, with a focus on computerised sensing component control [4]. To define the underlying standards, examples of commercial accelerometer ICs and exploration models will be used.

III. RESULTS AND DISCUSSION

Accelerometers are detecting gadgets that action a moving items speed increase and can identify recurrence and force of human development. For a really long time, accelerometers have been generally utilized in checking useful engine development, remembering reads up for neuromuscular issues like stroke and Parkinson's infection, and have zeroed in on estimating walk, stance, and quake boundaries, as well as identifying falls. Body-worn accelerometers have additionally been used to group exercises in sitting, strolling, standing, cycling, and lying positions, and have shown high exactness's in such examinations [5]. Moreover, accelerometers have been utilized to gauge the gross measure of arm development for furthest point recovery; in any case, it can't follow finger development, for example, getting a handle on, making it inadmissible for following developments engaged with ADL given that getting a handle on is a motion basic to activities, like holding and lifting objects. Considering that accelerometers are little and minimal expense, they have been planned and coordinated into numerous wearable advances, ordinarily formed into watches, wristbands, and groups, simple to wear clothing that can interest end-clients for ceaseless and long-haul use.

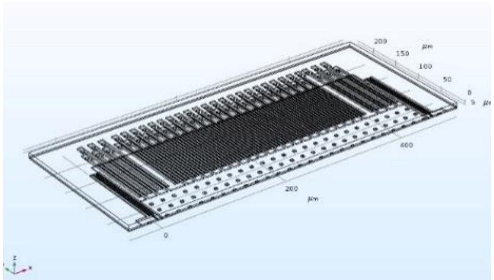

Fig 1.2 Component

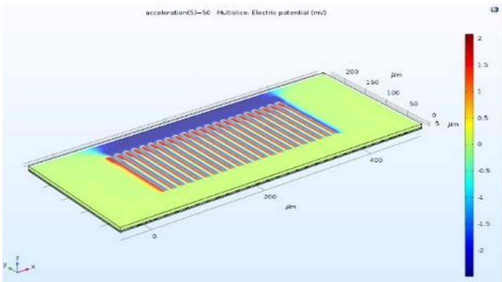

Fig 1.3 Surface displacement

The SAM is made out of a delivered confirmation proof-mass upheld by secured springs at its two closures, along with detecting and individual test cathodes reaching out to the sides. At the point when the gadget is dependent upon a speed increase, the reestablishing power gives a removal of the evidence mass in relation to speed increase. The uprooting leads to an adjustment of capacitance in between the fixed and moving cathodes. So this adjustment of the capacitance may be estimated it with various circuits [6].

Removal of polysilicon areas removing 0 V is applied to the decent individual test anode on the left side of the movable cathode connected to the mass of evidence and to 2V to the right. A confirmation mass was moved by about 0.02 μm sufficiently large in the size of the individual test base (contrasted with the 0.07 μm of full reach removal shown in **Fig1.2 and Fig1.3**)

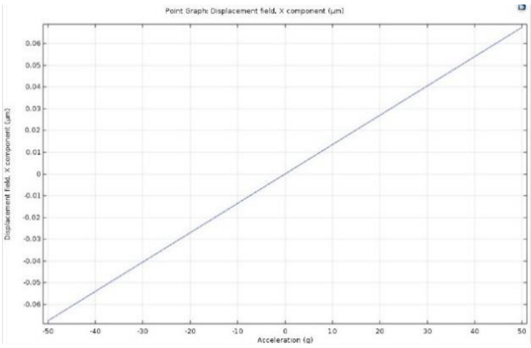

Fig 1.4 Displacement vs Acceleration

Fig 1.4 shows The SAM comprises of a side-extending detecting and self-test electrodes, as well as an open proof mass supported by springs fixed at both ends. The restoring force of the spring causes the proof mass to displace in accordance to the acceleration when the device is accelerated. [7]. The capacitance between the fixed and mobile electrodes changes as a result of displacement. Several conventional circuits can be used to measure the change in capacitance. There is a direct link between dislodging and the increased speed. The capacitance connection between decent anodes and movement is used to estimate dislodging. Confirmation proof of mass connected moving cathodes is drifting at a likelihood near half of the stockpile voltage, and a high recurrence square wave swinging from the genuine gadget on that time ordinary activity. The normal electrostatic power between the stationary and moving sensing cathodes is nullified in this scheme, and the linked hardware uses simpler sign handling. The fixed portion of the square wave is displayed using a fixed report in this paradigm, with the purpose of quickly addressing the issue. To reduce the electrostatic power between the fixed and moving sense terminals, the inclination is set to zero for comfort, and the abundant Ness of the square wave is isolated by a counterfeit element of 1000. (by and by the time normal of the power will be zero because of the great recurrence excitation). This compares to applying a +/- 2.5 mV on the right-side and left-side fixed senses for a 5 V stockpile in the actual device.

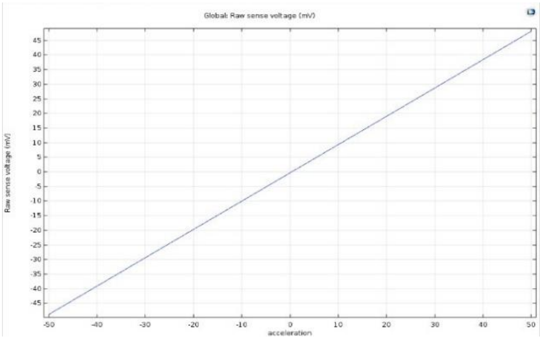

Fig 1.5 Applied acceleration versus Sensed voltage

Individual test anodes were built into the model accelerometer so that it could be fine-tuned on the assembly line. By applying a gradient of 2 to the appropriate individual test anodes installed along the edge of the movable anode on the confirmation mass, subsequent verification is defined as self-verification. The electrostatic force that moves the verification mass is applied by the electric field between the fixed and movable anodes. [9]. **Fig 1.6** shows When 0 V is delivered to the relevant individual test anodes on the left-hand side of the moving cathodes connected to the evidence mass, and 2 V to those on the right-hand side, the polysilicon regions uproot. In contrast to the 0.07 m of full reach relocation, the evidence mass moves by roughly 0.02 m, which is large enough for the individual test reason.

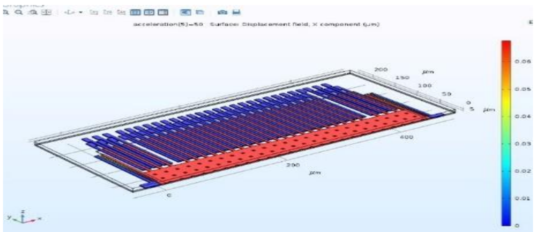

Fig 1.6 Displacement of the polysilicon

Fig 1.6 Displays displacement of polysilicon on domain when 0 V is applied to the fixed self-test electrode on the left side of the movable electrode mounted on the proof mass, and the right side 2V. Evidence is moved to about 0.01um, which is sufficient size sufficient for the purpose of being confident. [10].

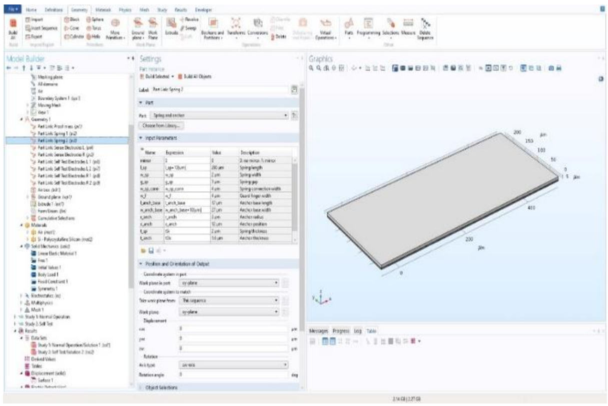

Fig 2.1 spring and anchor

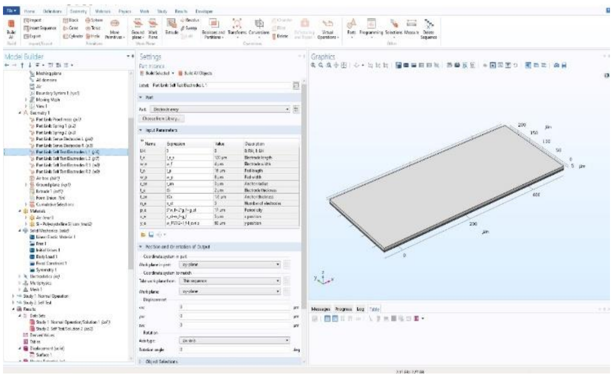

Fig 2.3 Parameter for Electrode array

The above **Fig 2.1** and **Fig 2.2** shows the parametric expressions for both string and anchor, electrode array respectively. The results will be different given parametric expressions we can add or delete expressions with respect to the required application.

IV. CONCLUSION

MEMS accelerometers in particular have ushered in a revolution in electronic gadgets, therefore in order to maintain accelerometer standards and stay up with evolving technology, MEMS accelerometers should now be designed using a variety of concepts and models for better results. Since the technology for MEMS-based accelerometer devices advances, the cost of manufacturing these devices falls dramatically, leading in the emergence of new markets. The developer's ingenuity is the sole limit to how these devices can be used. Furthermore, different groups are working to integrate three accelerometers and gyroscopes into a single box known as an inertial measurement unit (IMU), which will offer all of the data needed to reliably compute the positional controls required in many applications.

V. REFERENCES

[1] 'Robust LQR Controller Design for Stabilizing and Trajectory Tracking of Inverted Pendulum', 1877-7058 © 2013 The Authors. Published by Elsevier Ltd.

[2] 'Review of GPS Survey and GPS data',10.1080/01441647.2014.903530

[3] 'The Spring Loaded Inverted Pendulum as the Hybrid Zero Dynamics of an Asymmetric Hopper', August 17, 2007;

[4] 'Application of intelligent fuzzy PID controller Optimized by ALO Algorithm in AGC',978-1-7281-3361-4/19/$31.00 ©2019 IEEE

[5] 'A solution for study of PID controllers using cRIO System',978-1-4799-7514-3/15/$31.00 ©2015 IEEE

[6] 'Application of Neural Networks in Process Control', ISBN No. 978-1-4673-2048-1112/$3 1.00©20 12 IEEE.

[7] 'Design of Equivalent Fuzzy PID Controller from the Conventional PID Controller' 978-1-4673-9825-1/15/$3l.00 ©20 15 IEEE.

[8] 'Self-tuning PID Controller with Variable Parameters Based on Particle Swarm Optimization', 978-0-7695-4923-1/12 $26.00 © 2012 IEEE.

[9] 'Damping of Power System Oscillations by Using Unified Power Flow Controller with POD and PID Controller', 2014 International Conference on Circuit, Power and Computing Technologies [ICCPCT].

[10] '8-bit Efficient Digital PID Controller Architecture with Parallelism', IEEE May 19-20, 2017, India

[11] Design of Optimal PID [FOPID] controller for Linear system.10.1109/ICMETE.2016.45

[12] PID Implementation of Heating Tank in Mini Automation Plant Using Programmable Logic Controller (PLC) Corresponding Indispensable Subsidiary (PID)', Pahang, Malaysia, June 21-22, 2011.

[13] ‘Performance Analysis of Non-Integer Order PID Controller for Liquid Level Control of Conical Tank System’, ICICES2014 - S.A.Engineering College, Chennai, Tamil Nadu, India
[14] ‘Position Control of a 2DOF Rotary Torsion Plant Using a 2DOF Fractional Order PID Controller’, ‘Position Control of a 2DOF Rotary Torsion Plant Using a 2DOF Fractional Order PID Controller
[15] ‘Adaptive PID Controller Using for Speed Control of the BLDC Motor’, 2020 IEEE International Conference on Semiconductor Electronics (ICSE)
[16] ‘Hybrid Fuzzy PID Controller Design for a Mobile Robot’, IEEE ICASI 2018- Meen, Prior & Lam (Eds)
[17] ‘Fractional order fuzzy PID controller for a rotary servo system’, IEEE Conference Record: # 42666; IEEE Xplore ISBN:978-1-5386-3570-4
[18] ‘Comparative Analysis of robustness of optimally offline tuned PID controller and fuzzy supervised PID controller’, University Chandigarh, 06 - 08 March, 2014
[19] ‘MEMS Accelerometer based Digital Pen Recognition using Neural Networks’, Vol.2, Special Issue 1, March 2014.
[20] ‘Development of a behavioural model of the MEMS accelerometer’10.1088/1742-6596/1862/1/012010
[21] ‘Humanoid Robot Posture-Balance Control’, Proceedings of the SICE Annual Conference 2016 Tsukuba, Japan, September 20-23, 2016
[22] ‘Discrepancy Minimization via a Self-Balancing Walk’ STOC ’21, June 21–25, 2021, Virtual, Italy.
[23] ‘Modelling of a Balancing Robot on a Rolling Pipe’, ICCAE '18, February 24--26, 2018, Brisbane, Australia.
[24] ‘An automatic speech detection architecture for social robot oral interaction’, AM15, October 07-09, 2015, Thessaloniki, Greece.
[25] ‘Optimal path planning for two-wheeled self-balancing vehicle pendulum robot based on quantum-behaved particle swarm optimization algorithm’, 18 January 2019 /Accepted: 26 March 2019.
[26] ‘Control of a self-balancing robot driven by DC motors via IDA-PBC’, ICCMA 2017, October 11–13, 2017, Edmonton, AB, Canada.
[27] ‘A Single-ball-driven self-balancing robot controller based on genetic algorithm optimization’, AIAM 2020, oct-15-17-2020.
[28] ‘Dynamic Surface Active Disturbance Rejection Control for Two-Wheeled Self-Balancing Robot’, ICRCA '18, August 11–13, 2018, Chengdu, China.